

Contribution of a non-uniform magnetic field on the electric power of a photovoltaic panel

Kapim Kenfack Abraham Dimitri, Konga Eric and Pelap François Beceau*

UR de Mécanique et de Modélisation des Systèmes Physiques (UR-2MSP), Faculté des Sciences,
Université de Dschang, BP 69 Dschang, Cameroun.

* E-mail of the corresponding author: fbpelap@yahoo.fr and francois.pelap@univ-dschang.org

Abstract

Following existing studies on the effects of the uniform magnetic field conducted on a PV module, we note that the effect of a non-uniform magnetic field has not yet been conducted on a PV panel due to its large dimensions. In this paper, the behavior of a PV panel submitted to a non-uniform magnetic field is examined. The simplified synoptic of our PV panel is consisting of two large identical PV modules connected in series. By solving the continuity equation, we determine the distribution of minority carriers in this PV panel. Therefore, the output electrical characteristics (photocurrent, photovoltage and electric power) of this PV panel suggested to the effects of a non-uniform magnetic field are evaluated. In the standard test conditions, numerical simulations are carried out on the evolution of these electrical parameters. Our results show that a non-uniform magnetic field creates a non-uniform distribution of the electrical quantities in a PV panel. Moreover, we establish that, under the effects of a non-uniform magnetic field, the PV panel behaves as a PV panel suggested to the effect of partial shading. A comparative study between the impacts of a non-uniform and a uniform magnetic field on the PV panel is also carried out. It appears that a non-uniform magnetic field reduces the electric power of a PV panel more than a uniform magnetic field.

Keywords: Photocurrent; photovoltage; electric power; non-uniform magnetic field; PV panel; Shading.

DOI: 10.7176/JETP/10-7-03

Publication date: November 30th 2020

1. Introduction

It is well-known that a solar cell is one of several transducers, capable of directly converting the solar energy into electrical energy. It results from the pooling of a semi-conductor N doped (rich in electrons), with that P doped (poor in electrons). Regarding its genesis, the solar cell was first developed in 1954 and reaches an electrical efficiency of 6% around 1957. In those days, because of its low efficiency, it could not yet compete with non-renewable source of energy (fossils, charcoal, etc.). Nowadays, it has improved remarkably, and appeared as a sustainable alternative. In this perspective, the researchers paid great attention to the solar cell in the vein of postponing its sustainability. Thus, several of its parameters were studied in the aim of increasing its efficiency (Toure *et al.*, 2012; Diao *et al.*, 2014). Within these characterizations of the PV cell, it clearly appears that the external electrical field (Zerbo *et al.*, 2015), the light intensity (Mrabti *et al.*, 2009) and the nonlinearity (Dongo *et al.*, 2014; Pelap *et al.*, 2016) positively contribute to this efficiency while the temperature (Tyagi *et al.*, 2012; Pendem and Mikkili, 2018), the doping rate (Sane and Barro, 2015), the shading (Ekpenyong and Anyasi, 2013), the relative humidity of the site (Panjwani and Narejo, 2014), the dust (Sulaiman *et al.*, 2011) as well as the external magnetic field (Zerbo *et al.*, 2015) negatively act on this efficiency. By focusing our attention on the origins of the external magnetic field, we notice that it comes from several sources as shown in figure 1. The impacts of the external magnetic field in the scientific fields are diverse. On human health, it causes cerebral

hemorrhage, stress and blood cancer (Cihan *et al.*, 2016). In agriculture, the onion germination speed increases with the magnetic field (Hozayn *et al.*, 2015). The magnetic field impact is also present in other areas such as the damping modeling (Radhakrishnan, 2008), the magneto-mechanics (Mballa *et al.*, 2011), the electrical engineering (Zangui, 2011), the welding (Senapati and Mohanty, 2014) and the heat transfer (Vaux *et al.*, 2017). On the PV cell, the researchers studied the effect of a uniform magnetic field in order to optimize its photo conversion.

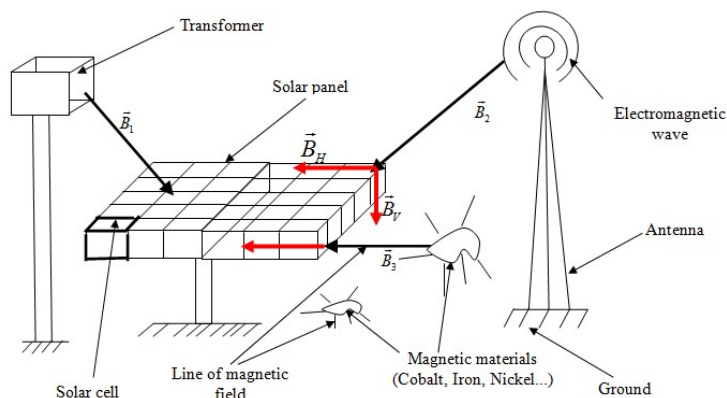


Figure 1: Presentation of a PV panel subjected to magnetic fields in a real situation

Thus, the solar cell is not affected by a magnetic field whose value is around $5 \times 10^{-5} T$ (Zerbo *et al.* 2015). Somewhere, when the magnetic field increases, the diffusion coefficient and length as well as the recombination effect decreases (Diouf *et al.*, 2016; Mane *et al.*, 2017). Latter, Cheikh *et al.* (2015) and Samb *et al.* (2010) showed that when the magnetic increases, the short-circuit photocurrent of a solar cell decreases while its open-circuit photovoltage increases. In the same vein, Zerbo *et al.* (2015) and Zoungrana *et al.* (2017) established that the electric power and the conversion efficiency of a solar cell decrease with the growth of the uniform magnetic field. It appears in all of the above-mentioned works that the effect of the uniform magnetic field was checked in the solar cell.

In the real conditions, the magnetic field is assimilated as uniform on a solar cell due to its smallness. In contrast, consider a magnetic field as uniform on a PV module, or PV system is absurd, because of their large dimensions. In fact, the magnetic field is a vector quantity which varies in direction and in intensity, as one moves away from its source. Furthermore, various sources of magnetic field can act simultaneously on a PV panel as shown in figure 1. Thus, a non-uniform magnetic field (coming from a single magnetic field or due to the superposition of various magnetic fields) can easily be created. Therefore we plan to investigate the effect of a non-uniform magnetic field on a PV panel.

This outline of this paper is structured as follows. In section 2, we present the model under study and examine theoretically the effects of a non-uniform magnetic field on a PV panel. Mathematical modeling of the system leads to the establishment of the analytical expressions of the photocurrent, photovoltage and electric power. In section 3, we consider the standard test conditions and carry out numerical investigations of the impact of the non-uniform magnetic field on the above-mentioned electrical parameters of a PV panel. Furthermore, a comparative study and discussion of the results obtained with the use of non-uniform and uniform magnetic fields are conducted. Section 4 is assigned to concluding remarks and recommendations.

2. Development of the model and characteristic equations

2.1. Description of the model

In the present study, the simplified synoptic of a PV panel consisting of two large identical PV modules connected in series is considered. Each PV module is made of N_p branches in parallel, each containing N_s identical solar cells connected in series. The diagram of the overview this PV panel is drawn in figure 2.

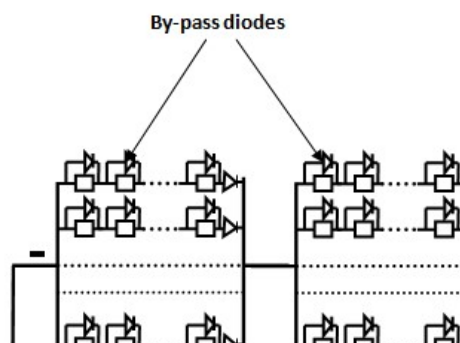


Figure 2: Simplified synoptic of a PV panel made of two identical PV modules connected in series. Each PV module consists of 10 branches in parallel; each branch contains 36 identical PV cells connected in series.

On figure 2, the quantities I and V designate, respectively, the current and the photovoltage delivered by the PV panel; V_1 and V_2 define the photovoltage at the terminals of the module 1 and 2, respectively. When the modules connected in series are identical, the parameters (electronics and electrical) of a PV panel can be easily determined. On this synoptic, protection diodes preserve the PV panel from the reverse current produced by the thunder during raining period. The bypass diodes provide an alternative route of current from a PV cell to another during the shading period, or when a PV module is partially destroyed.

However, when the electrical parameters are different in a PV panel, the electrical behavior is no longer easily predictable. In these perspectives, several mathematical models of such system have been proposed, aiming to calculate the effects of non-identical cells in a given module (Karatepe *et al.*, 2007; Ishaque *et al.*, 2011). Their works revealed that these differences between the solar cells in a given PV module dissipate the energy of the system by Joules effect, leading to the reduction of the electric power. To solve this dissipation problem, the parallel connection of a bypass diode to its terminals is recommended (Herrmann and Weisner, 2000). Therefore, the simplified synoptic of figure 2 is modified as displayed in figure 3, in which D_1 and D_2 represents the bypass diodes. These bypass diodes in this case ensure the continuity of current in a PV panel when a PV module is no more operating.

4. Conclusion

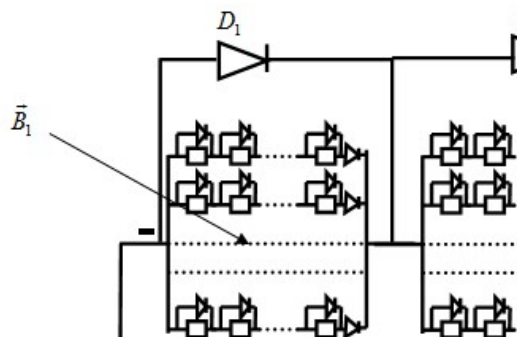


Figure 3: Modified synoptic of a PV panel suggested to a non-uniform magnetic field. The quantities D_1 and D_2 are the bypass diodes and V is the voltage across the PV panel.

In the real condition, depending on the magnitude, the angle of incident and the distance between the PV panel and the source of magnetic field as shown figure 1, the resultant of the magnetic field coming from the various sources will be different from a point to another on a PV panel. Thus, we get a non-uniform distribution of the magnetic field on a PV panel. Hence, we will simplify our study by considering the average values of the magnetic field on each PV module, such as the magnetic field is non-uniform on the whole PV panel. Then, B_j and θ_j are the average value of the magnetic field and its angle of incident on the j^{th} module, respectively. We assume that the lighting is uniform on the PV panel and that the generation rate of the carriers depends solely on the depth of the solar cell (Dieng *et al.*, 2011). This allowed us to conduct the study on a solar cell and then extend the results to the whole PV panel. We also assume that, the magnetic field acting on a PV panel is uniform on each module, but different from one module to another.

Each monocrystalline solar cell of the PV panel is presented in figure 4. The quantity H represents the thickness of a solar cell. In practice, the dimensions of the base along the x and y axes are very large compared to the depth of the solar cell. Hence, the current through these directions are negligible and the density of the carriers is uniform in the plan (Oxy) .

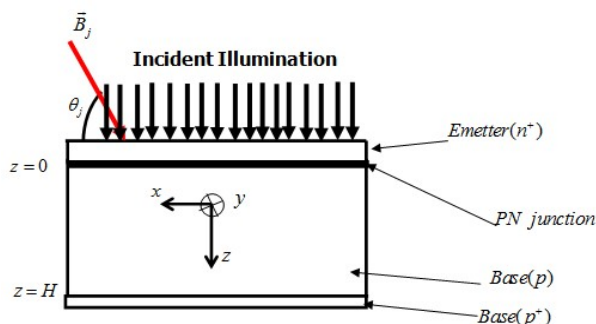


Figure 4: Description of the solar cell under the effect of both uniform external magnetic field and illumination

Throughout our investigations, we assume that the contribution of the emitter is negligible because of the smallness of its diffusion coefficient of the minority carriers compared to that of the base (Ly *et al.*, 2012). Therefore, the analysis is made in the base of each solar cell. The electrical parameters are supposed to be homogenous on each solar cell. We also suppose that, the generation rate of the carriers is linked to the thickness

of each solar cell.

2.2. Excess minority carrier density

The continuity equation for the minority carriers density δ_j generated in the base of the solar cell is expressed as follows (Diatta *et al.*, 2016; Diallo *et al.*, 2017; Diouf *et al.*, 2017):

$$\frac{\partial^2 \delta_j}{\partial^2 z} - \frac{\delta_j}{(L_j^*)^2} = -\frac{G(z)}{D_j^*} \quad (1)$$

wherein $G(z) = N \sum_{i=1}^3 a_i \cdot e^{-b_i z}$ defines the position depending on the generation rate of the carriers in which a_i , b_i , N are coefficients deduced from the generation rate modeling considered for over all the solar radiation spectrum (Ly *et al.*, 2012). The quantity $L_j^* = \sqrt{D_j^* \cdot \tau}$ represents the diffusion length of carriers of the j^{th} module in the presence of the magnetic field. Sourabié *et al.* (2017) established that the diffusion coefficient is function of the magnetic field and its angle of incidence varies randomly between 0 and $\pi/2$. Based on this work, we establish that the diffusion coefficient of the carriers in the j^{th} PV module is

$$D_j^* = D \left(1 + \mu_o^2 B_j^2 \sin^2 \theta_j \right) / \left(1 + \mu_o^2 B_j^2 \right) \quad (2)$$

in which μ_o , D are the intrinsic mobility of the carriers in the absence of magnetic field and the diffusion coefficient, respectively. The general analytical solution of Eq. (1) can be written as:

$$\delta(z, B_j, \theta_j) = M_j \cosh\left(\frac{z}{L_j^*}\right) + C_j \sinh\left(\frac{z}{L_j^*}\right) + \sum_{i=1}^3 \beta_{ij} e^{-b_i z} \quad (3)$$

in which we put $\beta_{ij} = -a_i (L_j^*)^2 / \left\{ D_j^* \cdot [b_i^2 (L_j^*)^2 - 1] \right\}$ are the matrix elements and the unknown coefficients M_j , C_j are obtained while exploiting the following boundary conditions (Ndiaye *et al.*, 2015):

- At the PN junction of the solar cell

$$D_j^* \frac{\partial \delta_j}{\partial z} = S_f \delta_j \quad , \quad z = 0 \quad (4a)$$

- At the back side of the solar cell

$$D_j^* \frac{\partial \delta_j}{\partial z} = -S_b \delta_j \quad , \quad z = H \quad (4b)$$

In expression (4a), the coefficient S_f designates the speed of recombination of the minority carriers at the space charge zone of the j^{th} PV module and defines the operating point of a solar cell. In this study, we consider the solar cell as ideal, assumption that allows the internal losses to be neglected in the analysis. Therefore, all the minority carriers that cross the PN junction will be collected (Zerbo *et al.*, 2015).

In relation (4b) the parameter S_b models the flux of the minority carriers effectively recombined on the rear face of a solar cell. This quantity is also called the speed of recombination and Samb *et al.* (2010) showed that it does not significantly affect the dynamics of a solar cell.

2.3. Photocurrent

In the case of a PV module (figure 3), only the parallel arrangement of the solar cells are involved in the photocurrent and consequently could induce a gain of photocurrent. The photocurrent delivered by each PV

module is linked to the speed of recombination. Base on the results obtained by Diallo *et al.* (2012), the mathematical expression of this photocurrent can be written as:

$$I_j(S_f, B_j) = q \cdot D_j^* \cdot \frac{\partial \delta_j(z, S_f, B_j)}{\partial z} \cdot N_p \cdot S_0 \Bigg|_{z=0} \quad (5)$$

in which S_0 and q stand for the area of each solar cell and the elementary charge, respectively. On the other hand, the two PV modules are connected in series, and the same current should normally flows through each of them. Therefore, the photocurrent delivered by the panel is expressed as follows:

$$I = \begin{cases} I_1 = I_2 & \text{if } D_1^* \cdot \frac{\partial \delta_1}{\partial z} = D_2^* \cdot \frac{\partial \delta_2}{\partial z} \\ I = \text{Max}(I_1, I_2) & \text{if } D_1^* \cdot \frac{\partial \delta_1}{\partial z} \neq D_2^* \cdot \frac{\partial \delta_2}{\partial z} \end{cases} \quad (6)$$

2.4. Photovoltage

As a PV module is concerned, only the series connection of the solar cells induces a gain of the photovoltage. Owing to the Boltzmann's law, the photovoltage across the PN junction of each PV module is expressed as (Ndiaye *et al.*, 2015):

$$V_j(B_j, S_f) = N_s \cdot V_t \cdot \log \left(1 + \frac{N_b}{n_i^2} \cdot \delta_j(z, B_j, S_f) \right) \Bigg|_{z=0} \quad (7)$$

where n_i , N_b are, respectively, the intrinsic concentration and impurity rate. The quantity $V_t = A \cdot K_b \cdot T / q$ represents the thermal voltage wherein A , T and K_b stand for the ideal factor, the temperature and the Boltzmann constant, respectively. Finally, the photovoltage at the outer charge terminals of the PV panel can be obtained as follows

$$V = \begin{cases} V_1 + V_2 & \text{if } D_1^* \cdot \frac{\partial \delta_1}{\partial z} = D_2^* \cdot \frac{\partial \delta_2}{\partial z} \\ \text{Max}(V_1, V_2) & \text{if } D_1^* \cdot \frac{\partial \delta_1}{\partial z} \neq D_2^* \cdot \frac{\partial \delta_2}{\partial z} \end{cases} \quad (8)$$

2.5. Electric power

By making use of relations (7) and (8), the general expression of the electric power provided by the PV panel of figure 3 could be written as (Zerbo *et al.*, 2016; Zoungrana *et al.*, 2017):

$$P = \begin{cases} (V_1 + V_2) \cdot I & \text{if } D_1^* \cdot \frac{\partial \delta_1}{\partial z} = D_2^* \cdot \frac{\partial \delta_2}{\partial z} \\ \text{Max}(V_1, V_2) \cdot I & \text{if } D_1^* \cdot \frac{\partial \delta_1}{\partial z} \neq D_2^* \cdot \frac{\partial \delta_2}{\partial z} \end{cases} \quad (9)$$

Equation (9) reveals that the electric power also depends on the speed of recombination of the minority carriers at the PN junction.

3. Results and Discussion

3.1. Effects of a non-uniform magnetic field on the output electrical parameters of a PV panel

In this subsection, we intend to investigate the impacts of a non-uniform magnetic field on each output electrical characteristics (known as the photocurrent, the photovoltage and the electric power) of a given PV panel made of two PV modules. Fortunately, the MATLAB software offers the possibility to carry out these numerical findings. These numerical investigations are done in standard test conditions where the irradiation is normalized at $0.1Wcm^{-2}$ and the temperature is $25^{\circ}C$. The following system parameters are exploited throughout this paper:

$$S_b = 100cm/s, S_0 = 7.5cm^2, \tau = 10^{-5}s, \mu_0 = 1500cm^2/Vs, \\ B_1 = 0.1mT, B_2 = 6mT, \theta_1 = \pi/3, \theta_2 = \pi/12, N_p = 10, \\ N_s = 36 \text{ and } H = 0.03cm, A = 1.2. \quad (10)$$

We treat the case of a monocrystalline silicon PV panel justified by the value of ideal factor A .

3.1.1. Effects on the photocurrent

In the scientific literature, Combari *et al.* (2017) studied the dynamics of a very small PV module having 36 cells connected in series. They considered a magnetic field as uniform on this PV module due to its small size. They showed that this PV module delivers a single short-circuit photocurrent which decreases with the magnetic field. However, to extend this study to a given PV panel, we should notice that the magnetic field over the entire PV panel will not be treated as uniform due to the large dimensions of the system.

In this subsection, the profile of the photocurrent delivered by the PV panel in terms of the speed of recombination S_f is obtained by exploiting (6) with the system parameters (10). For better understanding, the PV module **1** is subjected to a magnetic field $B_1 = 0.1mT$ and its angle of incidence $\theta_1 = \pi/3$ while the PV module **2** is under the couple $(B_2 = 6mT ; \theta_2 = \pi/12)$. The results obtained from simulation are displayed in figure 5. It appears from these curves that the photocurrent is almost nil for a very low recombination speed and it corresponds to the open circuit.

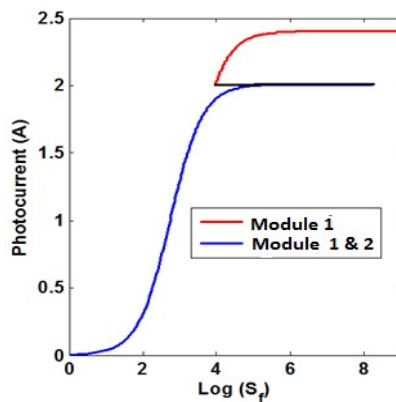


Figure 5: Photocurrent of a PV panel versus the speed of recombination, with the system parameters (10). A non-uniform magnetic field induces the birth of two short-circuit photocurrents in a PV panel, compared to the case of a uniform magnetic where only one short-circuit photocurrent is obtained.

Here, the PV panel does not produce current because no carrier is collected. These curves also reveal that the

photocurrent is maximal for large recombination speed and it corresponds to the short-circuit photocurrent. Furthermore, the PV panel exhibits two short-circuit photocurrents compared to the results established by Combari *et al.* (2017) showing only one. Indeed, under a non-uniform magnetic field, the parameters (electronic and electrical) of the two PV modules are different, due to the different levels of the average value of the magnetic field on each PV module.

The blue curve of figure 5 reflects the fact that the current produced by the PV panel is less than the short-circuit currents produced by each PV module. In this state, the two PV modules are operational and the same current flows in each of them. The minority carriers are extracted from the PN junction of each PV module with different speed of recombination, so that they produce the same output current. Since the PV module 2 possesses the smallest short-circuit photocurrent, it is first short-circuited. When the output current of the PV panel is beyond the short-circuit photocurrent of the PV module 2, the latter will dissipate the energy of the PV panel by joule effect. Therefore, the PV module 2 is automatically disconnected and the bypass diode D_2 across it becomes active to ensure the continuity of the current in the PV panel. Hence, the speed of recombination of the PV panel changes at constant current as shown the black horizontal line (figure 5) and falls in the zone plotted with the red color. In this zone, only the PV module 1 operates up to the maximum current produced by the PV panel as indicated on the curve.

3.1.2. Impact on the photovoltage

In this subsection, the profile of the photovoltage as function of the speed of recombination is plotted under the effects of a non-uniform magnetic field and displayed on figure 6. These curves are obtained by exploiting (8) with the system parameters (10).

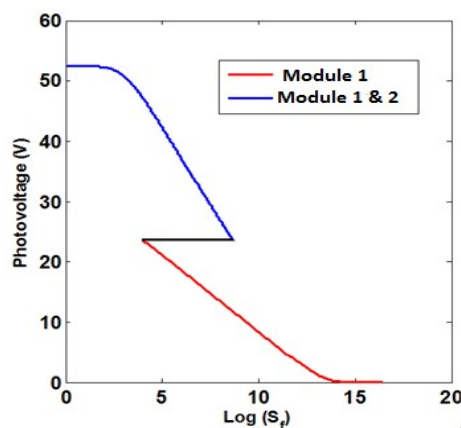


Figure 6: Photovoltage of a PV panel versus the speed of recombination with the parameters of figure 5. The curve presents two open circuit photovoltages

The graphs of figure 6 display three zones of different colors (blue, black, red). On the blue color curve, the photovoltage of the PV panel starts around $52V$ for low recombination speeds. This photovoltage corresponds to the open circuit photovoltage of the PV panel. In this blue zone, PV module 1 and 2 operate simultaneously. The photovoltage of the PV panel is the sum of the photovoltage delivered by each PV module. However, because the PV module 2 is more affected by the non-uniform magnetic field, it will be first shorted and disconnected. Then, we note a change of recombination speed with constant photovoltage as depicted in black color. From

there, only the PV module 1 will continue to operate and contribute to the production of photovoltage of the PV panel.

3.1.3. Consequences on the electric power

This subsection examines the evolution of the electric power in terms of the recombination speed for a PV panel suggested to the effects of a non-uniform magnetic field. Figure 7 exhibits the results obtained by exploiting expression (9).

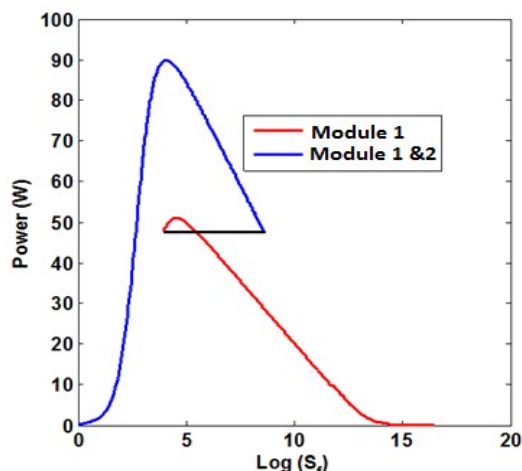


Figure 7: The electric power of a PV panel as function of the recombination speed. This curve presents two maximum electric powers, as in the case of the shading effect studied on a PV system by Ekpenyong and Anyasi (2013).

It clearly appears from this plot that the electric power is null for a low and high recombination speeds. Furthermore, the curve shows two maxima electric powers located at the intermediate operating point. In fact, on the blue curve, the two PV modules operate leading to a high electric power (91W). Whereas on the red curve, only the PV module 1 works, giving a low maximum power (52W). Thus, a non-uniform magnetic field applied on a PV panel induces the appearances of the multiple maxima of electric powers, as in the case of shading phenomena studied by Ekpenyong and Anyasi (2013). Facing this multiple peaks of power, the maximum power point tracking (MPPT) algorithm should not only scrupulously takes into account the shading phenomena, but also the effect of a non-uniform magnetic field on a PV panel. Thus, the global power could be extracted from a PV panel, and then satisfied the energy demand.

3.2. Comparative study on the effects of non-uniform and uniform magnetic fields on the PV panel outputs

In this section, we compare the effects of a uniform magnetic field and those of a non-uniform magnetic field on the electric output characteristics of a given monocrystalline silicon PV panel made of two different PV modules 1 and 2. The concerned characteristics are the photocurrent, the photovoltage and the electric power. Let us remind that in the case of a uniform magnetic field, we have $B_1 = 0.1mT$ and its angle of incidence $\theta_1 = \pi/3$, while for a non-uniform magnetic field situation, the PV module 1 is subjected to a magnetic field ($B_1 = 0.1mT$; $\theta_1 = \pi/3$) and the PV module 2 is under the effect of the couple ($B_2 = 6mT$; $\theta_2 = \pi/12$). The system parameters considered throughout this section are defined by relations (10).

In this subsection, we present a comparative study between the effect of a uniform and non uniform magnetic field applied to a PV field. This comparison is made on the photocurrent delivered by a PV field. These curves are obtained for the cases of a uniform and non-uniform magnetic field applied to a PV field. The results of our simulations are displayed on figure 8

3.2.1. On the Photocurrent

In this subsection, the comparison is carried out on the photocurrent delivered by a PV panel and the results of our simulations are drawn in figure 8. These curves are obtained for the cases of a uniform (red color) and non-uniform magnetic (black color) fields applied to a PV panel.

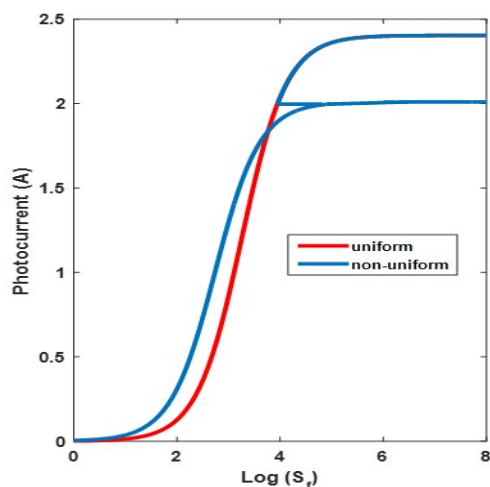


Figure 8: Photocurrent in terms of the speed of recombination under the effect of non-uniform and uniform magnetic fields for the parameters of figure 5. A single short-circuit photocurrent is obtained in the case of a uniform magnetic field compared with the case of a non-uniform magnetic in which two are viewed.

In the case of a uniform magnetic field, we notice the existence of only one short-circuit photocurrent while the non-uniform magnetic field case deals with two short-circuit photocurrents. In the first case, we recover the results established by Combarry *et al* (2017). In the second case, the actions of the two magnetic fields are superimposed. Furthermore, under a uniform magnetic field, all the PV modules converge towards the same short circuit whereas for a non-uniform magnetic field, each PV module converges toward its proper short circuit photocurrent. Thus, depending on the distribution of the magnetic field applied on the simplified synoptic of a PV panel panel, all the PV modules will operate or just only one will act.

3.2.2. On the photovoltage

In this subsection, results related to the behavior of the photovoltage of the PV panel suggested to the uniform and the non-uniform magnetic fields, respectively, are presented and compared. The system parameters are defined by (10) and the results of the simulations are summarized in figure 9. Indeed, in the two cases of (uniform and non-uniform) magnetic fields, we observe that the open circuit photovoltages of the PV panel are different. We also notice that both PV modules simultaneously contribute fully to the production of the photovoltage in uniform case, while after sometime in the non-uniform case, the PV module 2 stops operate. Furthermore, the PV panel offers a better photovoltage in the case of a uniform magnetic for a speed of

recombination beyond 10^9 cm/s , showing that the non-uniform magnetic field is very harmful for a PV panel. Then, from the above mentioned results, we could recommend manufacturers and engineers in charge of building and installing PV panels to also consider the effects of the non-uniform magnetic field in the region. Their work should contribute to minimize the different level of magnetic fields acting on a given PV panel. Thus, the losses in term of voltage should not be significant.

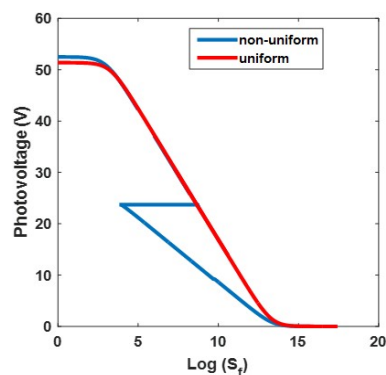


Figure 9: Photovoltage versus speed of recombination under the effect of a non-uniform and uniform magnetic field

3.2.3. On the electric power

This part presents a comparative study between of the effect of a uniform magnetic field and non-uniform magnetic field on the electric power delivered by a PV panel. The results are obtained with the parameters of figure 8 and displayed in figure 10.

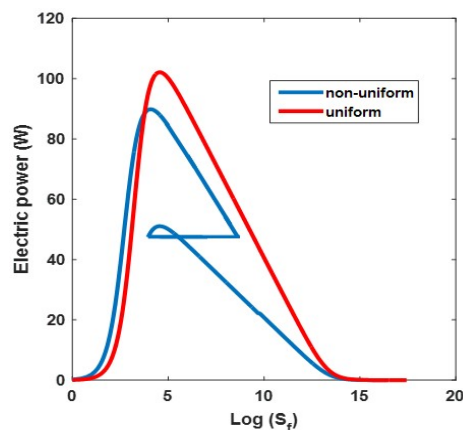


Figure 10: Electric power as function of the speed of recombination for a PV panel under the effects of both non-uniform and uniform magnetic fields. A uniform magnetic field offers a better maximum electric power ($P_{\max} = 103W$) compared to a non-uniform magnetic field ($P_{\max} = 91W$)

These curves allow noting that in the case of a uniform magnetic field, the PV panel delivers a single maximum electrical power of $P_{1\max} = 103W$ while in the case of a non-uniform magnetic field, two maximum electrical powers ($P_{21\max} = 91W$ and $P_{22\max} = 52W$) are obtained. These two last maximum powers are less than the single electrical power supplied under the uniform magnetic field. Therefore, we recommend to engineers that the PV panels must be installed in the area where the variation of the magnetic field is not significantly notable, in the vein to get a better electrical power.

4. Conclusion

In this paper, we examined the effects of a non-uniform magnetic field on a given PV panel consisting of two large identical monocrystalline silicon PV modules. Both analytical and numerical investigations on the behavior of the output electrical characteristics (photocurrent, photovoltage, electric power) of a PV panel are carried out. Many important results are established. First, it appeared that the non-uniform magnetic field induces the production of two short-circuit photocurrents, two open circuit photovoltages and two maximum electric powers. Moreover, our results revealed the PV panel under non-uniform magnetic field behaves like a PV module under the effect of partial shading (Ekpenyoung and Anyasi, 2013). During the comparative studies of the PV panel suggested to both uniform and non-uniform magnetic field, the behaviors of the electrical characteristics of the PV panel revealed that a non-uniform magnetic field is more harmful for a PV panel compared to a uniform magnetic field. As recommendations, manufacturers and engineers working on PV panels should take into account the harmful effects of the non-uniform magnetic field by minimizing the different levels of magnetic fields acting on PV panels. Thus, the PV panels must be installed in the area where the variation of the magnetic field is not significantly notable, in the vein to get a better electrical power.

References

- Cheikh, M.L.O., Seibou, B., Moujtaba, M.A.O., Faye, K., Wade, M., Sissoko, G. (2015). Study of base doping rate effect on parallel vertical junction silicon solar cell under magnetic field. *International Journal of Engineering Trends and Technology*, **19**, 44-55.
- Cihan, M., Eker, B. (2016). Magnetic Field Effects on Quality of Human Life. International conference on Quality of Life. 261-266.
- Combari, D.U., Zerbo, I., Zoungrana, M., Ramde, E.W., Bathiebo, D.J. (2017). Modeling study of magnetic field effect on the performance of a silicon photovoltaic module. *Energy and Power Engineering*, **9**, 419-429.
- Diallo, H.L., Dieng, B., Ly, I., Dione, M.M., Ndiaye, M., Lemrabott, O.H., Bako, Z.N. (2012). Determination of the recombination and electrical parameters of a vertical multifunction silicon solar cell. *Research Journal of Apply Science Engineering Technology*, **4**(16), 2626-2631.
- Diallo, M.M., Tamba, S., Seibou, B., Cheikh, M.L.O., Diatta, I., Ndiaye, E.H., Traore, Y., Sarr, C.T., Sissoko, G. (2017). Impact of illumination on the surface recombination velocity of a back side monochromatic illuminated bifacial silicon solar cell under frequency modulation. *Journal of Scientific Engineering Research*, **4**(1), 29-40.
- Diao, A., Thiam, N., Zoungrana, M., Sahin, G., Ndiaye, M. (2014). Diffusion coefficient in solar cell applied magnetic field and under frequency: electric equivalent circuits. *World Journal of Condensed Matter Physics*, **4**, 84-92.
- Diatta, I. Ly, I. Wade, M. Diouf, M.S. Mbodji S. Sissoko, G. (2016). Temperature effect on capacitance of a silicon solar cell under constant white biased light. *World Journal of Condensed Matter Physics*, **6**, 261-268.
- Dieng, A., Thiam, N., Thiam, A., Maiga, A.S., Sissoko, G. (2011). Magnetic field effect on the electrical parameters of a polycrystalline silicon solar cell. *Research Journal of Applied Science Engineering Technology*, **3**(7), 602-611.
- Diouf, M.S., Ly, I., Wade, M., Diatta, I., Traore, Y., Ndiaye, M., Sissoko, G. (2016). Study of the series resistance of a solar cell silicon under magnetic field from of junction surface recombination velocity of minority charge carriers at the junction limiting the open circuit (sfoc). *Journal of Scientific and Engineering Research*, **3**(6), 289-297.
- Diouf, M.S., Sahin, G. Thiam, A. Ngom, M.I. Faye, K. Gaye, D. Sissoko, G. (2017). Capacitance Voltage Characterization of Bifacial Silicon Solar Cell: Effect of External Electric Polarization. *Current Trends in*

- Technology and Science*, **5**, 669-672.
- Dongo, P.D., Kapim, A.D., Pelap, F.B. (2014). Effects of a thermal nonlinear resistance on the power output of the PV cell. *Journal of Energy and Technologies Policy*, **4**, 100-111.
- Ekpenyong, E.E., Anyasi, F.I. (2013). Effect of Shading on Photovoltaic Cell. *Journal of Electrical and Electronics Engineering*, **8**, 01-06.
- Herrmann, W., Weisner, W. (2000). Modeling of PV modules-The effect of non-uniform irradiation on performance measurement with solar simulators. 16th European Photovoltaic Solar energy conference 1-5 May.
- Hozayn, M., Amal, A.A., Rahman, H.M.H. (2015). Effect of magnetic field on germination seedling growth and cytogenetic of onion (ALLIUM CEPA.L). *African Journal of Agriculture Research*, **10**, 849-857.
- Ishaque, K., Salama, Z., Taheri, H., Syafaruddin. (2011). Modeling and simulation of photovoltaic (PV) system during partial shading based on a two-diode model. *Simulation Modelling Practice and Theory*, **19**, 1613-1626
- Karatepe, E., Boztepe, M., Olak, M.C. (2007). Development of a suitable model for characterizing photovoltaic arrays with shaded solar cells. *Solar Energy*, **81**, 977-992.
- Ly, I., Lemrabort, O.H., Dieng, B., Gaye, I., Gueye, S., Diouf M.S., Sissoko, G. (2012). Techniques de détermination des paramètres de recombinaison et le domaine de leur validité d'une photopile bifaciale au silicium polycristallin sous éclairage multi spectral constant en régime statique. *Revue des Energies Renouvelables*, **15**, 187-206.
- Mane, R., Ly, I., Wade, M., Datta, I., Douf, M.S., Traore, Y., Ndiaye, M., Tamba, S. Sissoko, G. (2017). Minority Carrier Diffusion Coefficient: Study in Temperature on Silicon Solar Cell under Magnetic Field. *Energy and Power Engineering*, **9**, 1-10.
- Mballa, F.S.M., Huberta, O., Lazrega, S., Meilland, P. (2011). Modélisation multidomaine du comportement magnéto-mécanique des aciers dual-phases, 20th mechanics french congress, Besançon (French), 29th August to 2nd September.
- Mrabti, T., Ouariachi, M.E., Tidhaf, B., Kassmi, Ka., Chadli, E., Kassmi, K. (2009). Modélisation des propriétés électriques et caractérisation des panneaux photovoltaïques. *Revue des Energies Renouvelables*, **12**, 105-116.
- Ndiaye, E.H., Sahin, G., Dieng, M., Thiam, A., Diallo, H.L., Ndiaye, M., Sissoko, G. (2015). Study of the intrinsic recombination velocity at the junction of silicon solar under Frequency modulation and illumination. *Journal of Applied Mathematics and Physics*, **3**, 1522-1535.
- Panjwani, M.K., Narejo, G.B. (2014). Effect of Humidity on the Efficiency of Solar Cell (photovoltaic). *International Journal of Engineering Research and General Science*, **2**, 499-503.
- Pelap, F.B., Dongo, P.D., Kapim A.D. (2016). Optimization of the characteristics of the PV cells using nonlinear electronic components. *Sustainable Energy Technologies and Assessments*, **16**, 84-92.
- Pendem, S.R., Mikkili, S. (2018). Modelling and performance assessment of PV array topologies under partial shading conditions to mitigate the mismatching power losses. *Solar Energy*, **160**, 303-321.
- Radhakrishnan, A. (2008). Effect of Magnetic Damping on Rotating Discs, *Bachelor Degree*, National University of Singapore, Singapore, 57pp.
- Samb, M.L., Zoungrana, M., Sam, R., Dione, M.M., Deme, M.M., Sissoko, G. (2010). Etude en modélisation à 3-D d'une photopile au silicium en régime statique placée sous un champ magnétique et sous éclairage multi spectral: détermination des paramètres électrique. *Journal des Sciences*, **10**, 23-38.
- Sane, M., Barro, F.I. (2015). Effect of both magnetic field and doping density on series and shunt resistance under the frequency. *Indian Journal of Pure Applied physics*, **53**, 590-595.
- Senapati, A., Mohanty, S.B. (2014). Effects of External Magnetic Field on Mechanical properties of a welded M.S metal through Metal Shield Arc Welding. *International Journal of Engineering Trends and Technology*, **10**, 297-303.

- Sourabié, I., Zerbo, I., Zoungrana, M., Combari, D.U., Bathiebo, D.J. (2017). Effect of incidence angle of magnetic field on the performance of a polycrystalline silicon solar cell under multispectral illumination. *Smart Grid and Renewable Energy*, **8**, 325-335.
- Sulaiman, S.A., Hussain, H.H., Leh, N.S.H.N., Razali, M.S.I. (2011). Effects of Dust on the Performance of PV Panels. *International Journal of Mechanical and Mechatronics Engineering*, **5**, 2028-2033.
- Toure, F., Zoungrana, M., Zouma, B., Mbodji, S., Gueye, S., Diao, A., Sissoko, G. (2012). The influence of magnetic field on electrical model and electrical parameter of a solar cell under intense multispectral illumination. *Global Journal of Sciences Frontier Research Physics and Space Sciences*, **12**, 51-59.
- Tyagi, V.V., Panwarb, N.L., Rahima, N.A., Kothari, R. (2012). Review on solar air heating system with and without thermal energy storage system. *Renewable and Sustainable Energy Reviews*, **16**, 2289-2303.
- Vaux, S.R.D., Zamansky, R., Bergez, W., Tordjeman, P., Haquet, J.F. (2017). Magnetoconvection transient dynamics by numerical simulation. *European Physical Journal E*, **40**, 1-13.
- Zangui, S. (2011). Détermination et modélisation du couplage en champ proche magnétique entre systèmes complexes. *PhD Thesis*, French. University of Lyon. 135p.
- Zerbo, I., Zoungrana, M., Sourabie, I., Ouedraogo, A., Zouma, B., Bathiebo, D.J. (2015). External magnetic field effect on bifacial silicon solar cell's electric power and conversion efficiency. *Turkish Journal of Physics*, **39**, 288-294.
- Zerbo, I., Zoungrana, M., Sourabie, I., Ouedraogo, A., Zouma, B., Bathiebo, D.J. (2016). External magnetic field effect on bifacial silicon solar cell's electrical parameters. *Energy and Power Engineering*, **8**, 146-151.
- Zoungrana, M., Zerbo, I., Soro, B., Savadogo, M., Tiedrebeogo, S., Bathiebo, D.J. (2017). The effect of magnetic field on the efficiency of a silicon solar cell under an intense light concentration. *Advance Science and Technology*, **11**, 133-138.